Antenna Performance in a Corona Plasma

Marcin M. Morys, and Gregory D. Durgin, Ph.D.

***Abstract*—The formation of corona discharges at high potentials was studied. Glow coronas were found to be generated when the electric field magnitude is in excess of 3MV/m in general for air at atmospheric pressure. The number density of electrons in the glow corona can only be approximated, but the results obtained from the Boltzmann transport equation promise to be accurate enough to give meaningful wave attenuation results, so long as the number density is below 10^{19} m^{-3} electrons. Above this density, the attenuation increases dramatically and approximations for density may no longer be valid. Wave propagation and antenna parameters in a corona plasma can be computed through simulation using dielectric slabs of complex impedance to simulate a plasma sheath.**

***Index Terms*—Smart grid, glow corona, plasma sheath, plasma frequency**

I. Introduction

An important area of research and development which is quickly gaining interest is power handling and distribution. The "Smart Grid," as it is referred to in public circles, is the constantly evolving system that entails the efficient, reliable, and secure distribution of power from numerous sources to the even more numerous customers. For decades, the technology involved in power transmission had been at a standstill with little innovation. Today, the need for an improved power grid is quickly rising as energy costs go up and the demand for reliable power multiplies [1].

A major advance in improving the efficiency of power distribution is the deployment of low cost sensors along transmission lines and throughout substations. These sensors can provide active monitoring capabilities for fast and easy management of the grid. Such sensors must often be placed in very close proximity to high voltage lines. One challenge that this poses is difficulty in transmitting information to a receiver. Physical connections through wires or fibers are dangerous because of the risk of creating a short to ground. The obvious solution is wireless data transmission.

A wireless solution is cheap, easy to install, safe, and adaptable to many applications. However, this does not come without its own difficulties. A sensor mounted on a high voltage line will itself be at a high potential. Depending on the voltage in question (typically in the hundreds of kV) and the geometry of the sensor, a corona plasma may form around the geometry due to the ionization of air. The free electrons in this corona will absorb electromagnetic energy radiated by the antenna through collisions, reducing the power at the receiver as well as possibly changing the characteristics of the antenna such as input impedance [2]. This report addresses the effect of a corona created by and surrounding a printed antenna at high potential.

II. Ionization Mechanics

Ionization is a process by which a gas molecule becomes an ion (charged particle), typically through the loss or gain of electrons. This process can be brought on and sustained through several mechanisms. In this report, we focus on ionization brought on by generating a strong electric field in a gas such as air. The electric field magnitude can be obtained by solving for Poisson's Equation in the geometry, taking the potential source and ground as boundaries.

$$\nabla \cdot \varepsilon \boldsymbol{E} = \rho$$

The basic mechanism for generating a corona plasma is the electron avalanche. To illustrate this process let us consider a basic geometry involving the two-dimensional coaxial cross section illustrated in Figure 1. The center wire is at a high potential V and the surrounding conductor is grounded. Solving for the electric field yields [3]

$$E(r) = \frac{V}{r \ln r_2/r_1}$$

where r_1 is the radius of the inner conductor and r_2 is the radius of the outer conductor. Assuming the voltage applied is steady DC and positive, a strong electric field will be present at the surface of the wire. If the magnitude of the electric field reaches a certain value, self-sustaining ionization will occur.

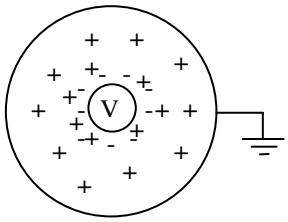

Fig. 1. Charged particle distribution in positive DC corona

The electron avalanche is a process whereby a free electron in a gas is accelerated over a distance, termed the free path, and collides with a molecule with great enough energy to dislodge a second electron. Both electrons are now accelerated by the field and collide with two more molecules, exciting their electrons out of their orbits bringing the net number of free electrons to four. This process continues until the

electrons arrive at the anode. The parameter defining this process is called Townsend's first ionization coefficient. It is defined as the number of electrons produced per unit length in the direction of the electric field, and is given by the following relation

$$\frac{\alpha}{P} = Ae^{-Bp/E}$$

where α is Townsend's first ionization coefficient, P is the gas pressure, E is the electric field magnitude, and A and B are constants. One can further derive an expression for the electron density in a given volume as

$$\frac{n}{n_o} = e^{\int_{x1}^{x2} \alpha \, dx}$$

where n is the electron number density, n_o is the electron density emitted by the cathode, and α is the spatially dependent ionization coefficient. For practical situations, this solution cannot be solved directly because of difficulties in accurately computing the ionization coefficient in non-uniform fields [3]. Once the ionization current gets to a certain point it jumps several orders of magnitude with little increase in the source potential to produce a phenomenon known as the self-sustaining discharge. The self-sustaining discharge is no longer reliant on the source electric field to maintain ionization, and in fact will continue to ionize even if the electric field decreases, known as hysteresis. The criterion for self-sustaining discharge is given by Townsend's breakdown criterion [3]

$$\frac{\alpha}{\beta} = e^{\alpha d}$$

where β is Townsend's second ionization coefficient, the number of electrons produced by ion-molecular collisions, and d is the distance from x_1 to x_2. The glow corona is a type of self-sustaining discharge which is of importance in this topic. Its constant high electron density near the surface of the anode can create issues in signal transmission when that anode is an antenna.

In most practical high voltage applications, the voltages are AC as opposed to DC. On first inspection, one may reason that the time-varying voltage will not affect the corona formation because the period of the voltage cycle is on the order of milliseconds while the time for electrons to reach the anode is on the order of microseconds. As such, one might presume that a static DC analysis for each instant in time in the cycle will suffice to model the charge distribution surrounding the structure. However, if the peak voltage is high enough to create a self-sustaining discharge, the hysteresis effect will cause a voltage signal time-dependent charge distribution [4],[5]. The effect can be visualized in Figure 2 produced by Carroll and Lusignan [6].

While the charge densities here are only accurate relative to an unknown constant, the offset of peaks from the applied voltage peaks is indicative of the tangible time delay there exists. For a rigorous calculation of charge density effects, the voltage frequency must be taken into account. However, for our study, we intend to study the effects of corona on antennas, and as such we can consider the worst case scenario of a DC corona to approximate the AC case behavior.

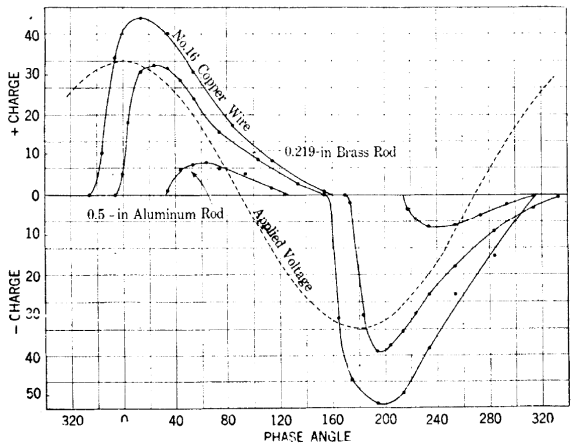

Fig. 2. Different diameter conductors at the center of a 15-in. cylinder. Applied voltage held constant for all three at 70kV

A general distribution of electrons and ions is shown in Figure 1 for a positive DC discharge. The electrons, having a small mass compared with ions, will be accelerated toward the anode and form a high density sheath near its surface. The effective radius of this electron sheath can be approximated for a coaxial geometry as well as a wire parallel to ground geometry using Peek's empirical formulas. The wire to ground geometry equations are given here because of their practical utility in power line to ground applications [7]

$$E_o = 2140\delta(1 + \frac{0.0301}{\sqrt{r\delta}})$$

$$V_o = E_o r \ln(\frac{2H}{r})$$

where E_o is the corona inception electric field strength (kV/cm), H is the line height above ground (m), r is the line radius (m), δ is a line roughness factor (=1 for smooth cylinder), and V_o is the corona inception voltage (kV, rms).

To obtain a practical estimate of the sheath radius and corona inception field strength, we can estimate a typical power line radius of 1cm and line height of 3m to get

V_o = 178kV, rms
r_o = 1cm

AC voltages as high as 500kV are used in the United States for long distance transmission, and we can see that corona development is possible, especially when the lines exhibit some roughness due to rain drops or wear. While we do gain some insight here into the orders of magnitude involved in glow corona development, we cannot yet estimate the number densities of electrons in the sheath.

III. Boltzmann Transport Model

The accurate calculation of electron number densities in a DC discharge plasma is a difficult task because of the many

variables involved in the process. Should one desire to rigorously compute the electron number density from the electric potentials on the boundaries, one would have to solve a series of coupled equations on a molecular level involving conservation of charge, energy, and momentum. Such a calculation, while computationally demanding, can be performed by software such as COMSOL Multiphysics. This project will attempt to utilize a simplified model for electron transport to obtain a reasonable estimate for their distribution.

Since we are dealing with individual electrons that, as a whole, behave like a fluid, the Boltzmann transport equation is an appropriate model for the situation. In [8], Fante derives the Boltzmann transport equation as it applies to electrons in a plasma.

$$\frac{dn}{dt} = -\nabla \cdot \Gamma + (\nu_i - \nu_a)n$$

Given here is the transport equation, where ν_i and ν_a are the ionization and attachment frequencies respectively, while the following is the current density

$$\Gamma = \langle V \rangle n - \mu E n - \nabla D n$$

The three terms in the current density represent convection, drift, and diffusion respectively. In addition, $\langle \boldsymbol{V} \rangle$ stands for the net velocity of the gas, μ stands for the electron mobility, and D stands for the electron diffusion coefficient.

According to [9], in a low frequency situation such as the 60Hz power line excitation, drift is the dominant mechanism in the current density, and diffusion can be ignored. With a higher frequency excitation such as with a microwave plasma, diffusion would dominate drift. In both situations we can ignore the velocity term. In reality this would have an effect on power lines, and can be taken into account at a later point to account for wind on the electron distribution.

In order to solve this differential equation over a boundary, the mobility and ionization rates must be provided. All values used in the computation of Boltzmann transport are is SI units. These are taken from empirically derived datasets and curve fit to obtain a functional form which can be used in the transport equation. Mobility data is obtained from [10] for dry air and atmospheric pressure and curve fit to give

$$\mu = 7.43 * (E + 57)^{-0.35}$$

The offset of 57 is used in the definition of mobility to limit it to finite values as the electric field goes to zero. A maximum mobility of 1.8 $m^2/v\,s$ is chosen from a study of electron mobility in Nitrogen at low field strengths [11]. The data and curve fit are illustrated in Figure 3.

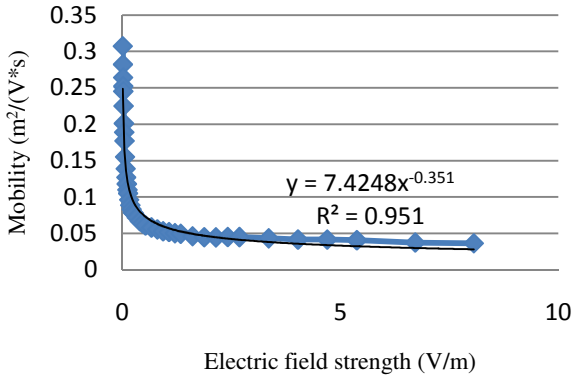

Fig. 3. Electron mobility in dry air at atmospheric pressure

The ionization and attachment rates for electrons to be utilized in the transport equation are obtained from [12]. Both rates are obtained from the experimental results for dry air and subtracted to get the net ionization rate before performing a curve fit. The original data curves are shown in Figure 4.

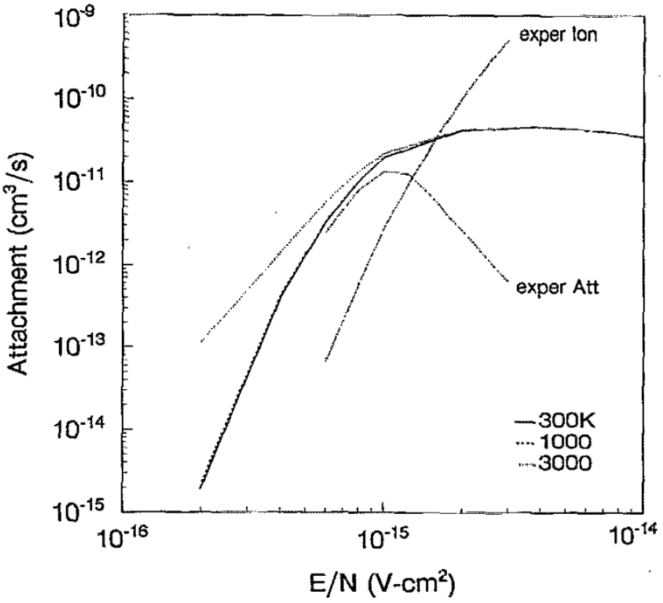

Fig. 4. Dry air ionization and attachment rates at atmospheric pressure

The data points for the net ionization $\nu_i - \nu_a$ and respective curve fit are shown in Figure 5. A value of N=2.688x10^{25} is used for the air number density in obtaining Figure 5 from Figure 4, i.e. convertion E/N to E and $\frac{(\nu_i - \nu_a)}{N} to\ \nu_i - \nu_a$.

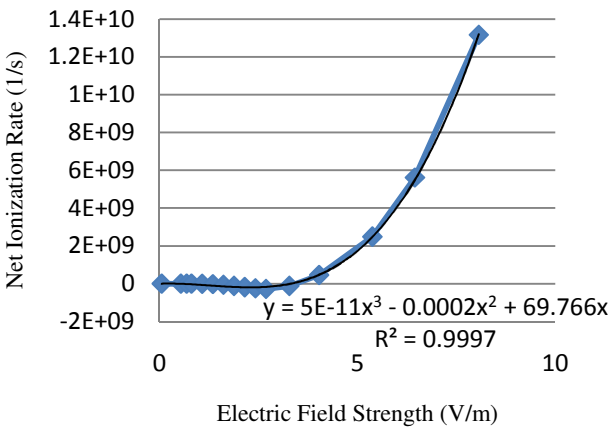

Fig. 5. Electron net ionization rate in dry air at atmospheric pressure

With functional values for the electron mobility and net ionization rate, the Boltzmann transport equation can be solved numerically. COMSOL Multiphysics is employed to this end. To simplify the model as much as possible, the geometry shown in Figure 1 is attempted first. The electric field solution is decoupled from the transport equation by assuming that the electron and positive ion densities are equal, thus allowing for a solution to Laplace's Equation. The voltage on the inner conductor is chosen large enough that the electric field magnitude near the conductor is greater than the generally accepted dielectric strength of air, $3\text{x}10^6$ V/m [13], assuring plasma formation. The equation is solved for the steady state where

$$dn/dt = 0$$

since this should give the electron density without performing a time dependent simulation. The software is unable to converge to a solution indicating that there is either an issue with the formulation of the transport equation, the curve fits to data seen above, or the boundary conditions (voltages of the inner and outer conductors). After many unsuccessful attempts to obtain a solution for the problem, the Boltzmann transport equation is simplified down using some approximations to try to find the issue. These simplifications can be found in the appendix. The transport equation appears to break down for fields less than the dielectric strength of air, necessitating negative electron concentrations to converge to a solution.

A more exact implementation of the Boltzmann transport equation is utilized by Chen and Davidson [13]. According the Chen and Davidson, the diffusion of electrons cannot be ignored in the calculations even at low frequencies. This implementation also takes into account the generation of positive and negative ions through ionization and attachment. The net charge is no longer assumed to be zero, so Poisson's Equation must be utilized and the field solved simultaneously with the transport equations. The coupled equations are now

$$\frac{dn}{dt} = -\nabla \cdot \Gamma + (\alpha - \beta) n_e \mu_e E$$

$$\nabla \cdot \left(\mu_p n_p E\right) = \alpha \mu_e n_e E$$

$$\nabla \cdot (\mu_n n_n E) = -\beta \mu_e n_e E$$

$$\nabla \cdot E = \frac{e}{\varepsilon_o}(n_p - n_n - n_e)$$

where

$$\Gamma = \langle V \rangle n - \mu E n - \nabla D n$$

$$\alpha = \frac{\nu_i}{\mu_e E} = 3.63 \times 10^5 e^{-1.68\times10^7/E}$$

$$\beta = \frac{\nu_a}{\mu_e E} = 1.482 \times 10^3 e^{-3.465\times10^6/E}$$

$$\mu_e = 1.2365 E^{-0.2165}$$

$$\mu_p = 2.0 \times 10^{-4}$$

$$\mu_n = 2.7 \times 10^{-4}$$

Additional boundary conditions must be used to account for the additional degrees of freedom. The first boundary condition is setting the current density at the inner conductor equal to a predefined value, in this case chosen as 2.55μA/cm as per [13].

$$\Gamma|_{r=a} = J(a)$$

The electron density at the outer edge of the plasma ($r=r_o$), which is the sheath radius given by Peek's formula, is set to the number of electrons generated through photoionization which we take to be 10^8 m^{-3} based on the provided results. The positive ion density on the inner conductor is 0 because they do not add to the surface current, while the negative ion density at r_o is taken to be 10^8 m^{-3}. Finally, the electric field magnitude at r_o is set to $3\text{x}10^6$ V/m as the standard dielectric strength of air.

The simulation does converge to a solution. However, the values of the densities that are computed do not reflect physical values because they contain negative numbers over some portions of the solution region. The electric field does reflect a reasonable distribution as shown in the elevation plot in Figure 6. This inconsistency in results is the current focus of ongoing research.

IV. Electromagnetic Propagation Through Plasma

Plasma is composed of free electrons and ions. As such, it can behave in a similar manner to a conductor. In order to simulate the attenuation of an electromagnetic wave through ionized air, it can be modeled as a lossy dielectric [14],[15]. Wei et al. give the complex plasma permittivity as

$$\varepsilon_p = \varepsilon_o \left[1 - \frac{{\omega_p}^2}{\omega(\omega - j\nu_c)}\right]$$

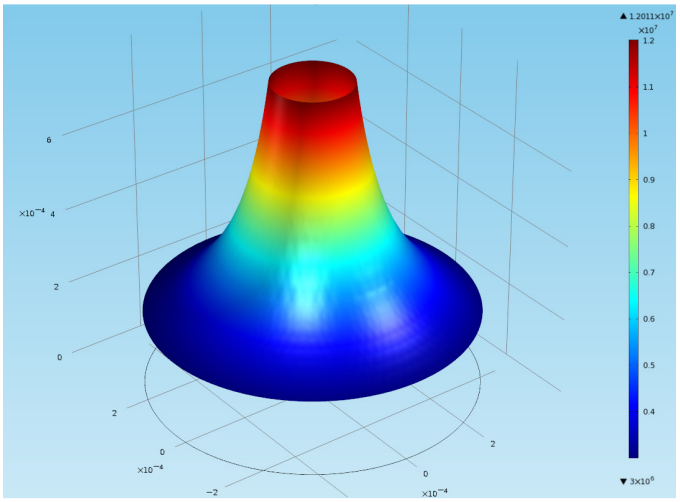

Fig. 6. Electric field magnitude for coaxial geometry with outer conductor grounded

where

$$\omega_p = \sqrt{\frac{e^2 n_e}{\varepsilon_o m_e}}$$
$$\nu_c = 10^9 Hz$$

are the plasma frequency and collision frequency respectively. A derivation of the plasma frequency from basic physics principles is given in the appendix. The plasma frequency is the frequency at which the bulk electron mass oscillates. It is derived by taking into account the dielectric dipole moment of the free electrons into the differential equations for electromagnetic wave propagation.

In a plasma with low density, the plasma frequency stands as a cutoff frequency between reflection and unattenuated propagation. Below ω_p the wave is completely reflected back and above ω_p the wave propagates through. However, at high gas densities such as in air at atmospheric pressure, the behavior of a plasma changes due to the high frequency of collisions between electrons [16]. Laroussi gives the collision frequency for air as

$$\nu_c = 10^{12} Hz$$

which is three orders of magnitude higher than that given by Liu. According to Laroussi, this high collision frequency causes the attenuation of the wave to increase with increasing frequency. The attenuation of an electromagnetic wave propagating through a slab of plasma with plasma frequency as stated above and collision frequency as given by Laroussi is

$$T(dB) = 20 \log_{10} e^{-\alpha \frac{d}{\cos \theta_t}}$$

$$\alpha = \frac{\omega}{c} X$$

$$\theta_t = \sin^{-1} \frac{\cos \psi}{\mu}$$

$$X = \sqrt{-\frac{1}{2} + \frac{1}{2}\sqrt{1 + \left(\frac{\omega_s}{\omega}\right)^2}}$$

$$\mu = \sqrt{\frac{1}{2} + \frac{1}{2}\sqrt{1 + \left(\frac{\omega_s}{\omega}\right)^2}}$$

$$\omega_s = \frac{{\omega_p}^2}{\nu_c}$$

T is the attenuation of the wave in dB, d is the thickness of the plasma slab, θ_t is the transmission angle, ψ is the grazing angle, i.e. complement of the incident angle, α is the attenuation coefficient, X is the attenuation index, μ is the refractive index, and ω_s is characteristic frequency. If an incident wave has a frequency higher than the characteristic frequency, the wave will be attenuated mostly by the transfer of energy to electrons which lose it to collisions with other particles. Below this frequency, the wave is mostly reflected back due to the phase shift between the force applied to the free electrons and their velocity vectors. It is a system where energy is absorb and reemitted back to its source each period of its oscillation.

The attenuation T of the wave is plotted in Figures 7-9 as a function of frequency, number density, and slab thickness assuming a 0^o angle of incidence. The base number density of electrons is approximated as 10^{19} m^{-3} from [14] and [17], the base slab thickness is 1cm as calculated from Peek's formula, and the base frequency is 5.8GHz.

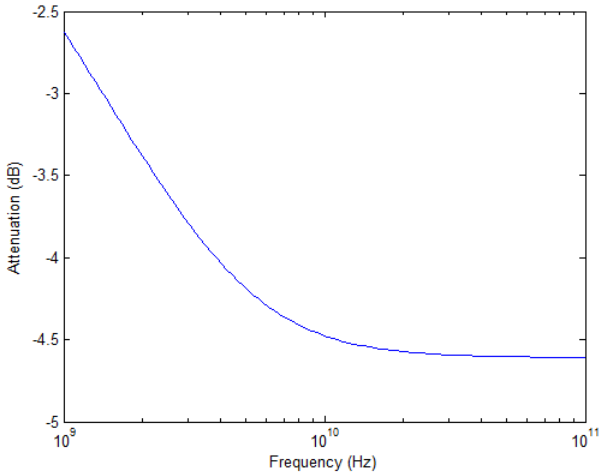

Fig. 7. Attenuation through a plasma slab with $n_e=10^{19}$ m^{-3} and d=1cm as a function of incident wave frequency

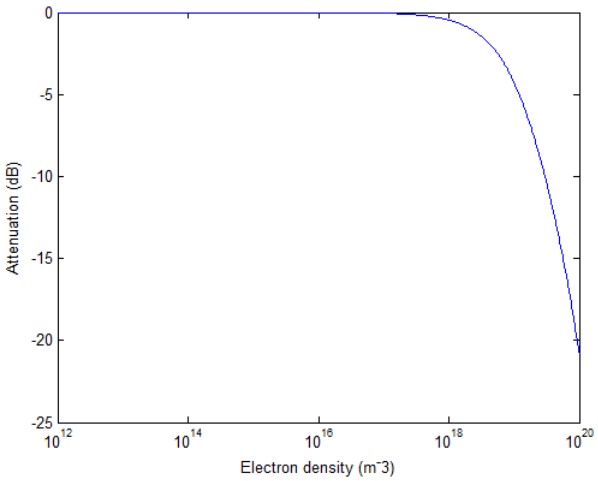

Fig. 8. Attenuation through a plasma slab with f=5.8 GHz and d=1cm as a function of incident wave frequency

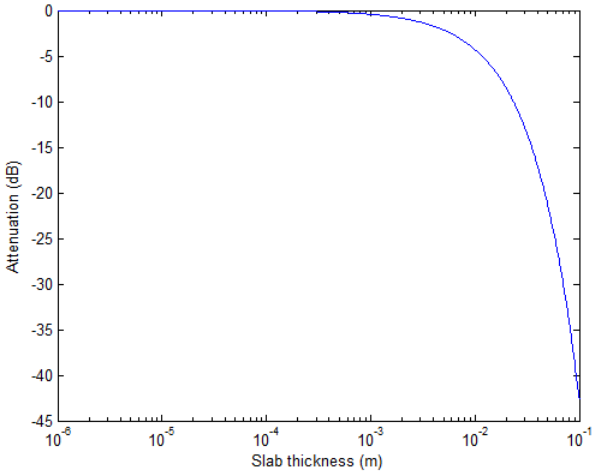

Fig. 9. Attenuation through a plasma slab with f=5.8 GHz and $n_e=10^{19}$ m^{-3} as a function of incident wave frequency

As is evident from Figure 7, it is desirable to minimize the frequency in order to minimize attenuation. Also, the attenuation undergoes a sharp spike around n_e=10^19 m^{-3} shown in Figure 8. It is crucial to ensure that the number of sharp corners and curves be minimized in the antenna geometry to minimize both the number density as well as the thickness of the corona. It should be noted that these plotted values are overestimates. The number density of a slab of plasma decreases rapidly with increasing distance from antenna at high potential[18], whereas here we assumed it is constant throughout.

V. Antenna Design Recommendations

It is clear that in order to minimize attenuation of the electromagnetic wave on its path from the tag to the reader, the electron number density and thickness of the plasma must be minimized. In order to accomplish this objective, it is critical that the electric field be as small as possible, meaning that the surfaces should be as flat or rounded. Shown in Figure 10 is an antenna at 500kV five meters above ground. With square corners, the electric field reaches 8MV/m and is capable of generating a corona plasma. In Figure 11 is shown the same arrangement, this time with rounded ends. This modification is enough to maintain the electric field below 3MV/m to prevent serious ionization.

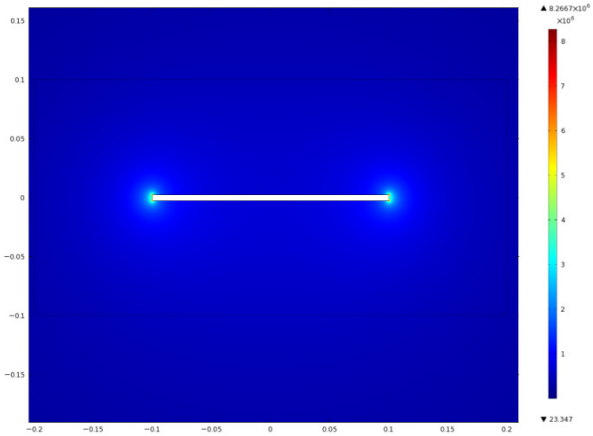

Fig. 10. Electric field from sharp antenna ends

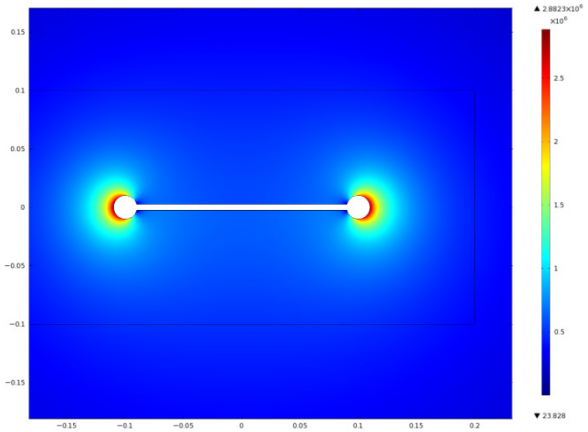

Fig. 11. Electric field from rounded antenna ends

To create an even more robust system, we recommend investigating horn antennas. Since the electromagnetic wave propagates inside a waveguide, the electric field will be very small in this volume given the waveguide walls are at the same potential. Tapering back the ends of the waveguide will minimize the fields at the edges to create an antenna the is robust against corona generation, even with the formation of sharp points on its surface due to rain or debris.

VI. Conclusions

Through an analysis of Peek's formula and the methods of ionization, we gained some insight into the causes and effects of DC glow discharges. A parametric analysis was performed for electromagnetic attenuation in a generic slab of plasma in air. Through this analysis, we discovered that the attenuation of an electromagnetic waves increases rapidly once the number density of the electrons reaches n_e~10^{19} m^{-3}. The Boltzmann model formulated for the electron and ion densities due to a positive DC discharge continues to give non-physical results. However, the same model was utilized by [19] to

obtain the electron density distribution for various DC discharges, so further analysis must be performed to discover the inconsistency in our methodology. Once the electron densities are correctly approximated for our antenna geometry, they can be modeled as lossy dielectric slabs and implemented in Ansoft HFSS to obtain new antenna parameters. The effect of the plasma can then be analyzed, and antenna designs can be improved in order to mitigate the effects of detuning due to plasma formation.

VII. Appendix

A. *Simplification of the Boltzmann transport equation*

$$\frac{dn}{dt} = \nabla \cdot (\mu n E) + \nu_{net} n$$

$$\frac{dn}{dt} \xrightarrow{steady\ state} 0$$

$$0 = \nabla(\mu n) \cdot E + \mu n(\nabla \cdot E) + \nu_{net}\, n$$

$$\nabla \cdot E \xrightarrow{0\ net\ charge} 0$$

$$0 = (\mu \nabla n + n \nabla \mu) \cdot E + \nu_{net}\, n$$

$$0 = \mu \nabla n \cdot E + n \nabla \mu \cdot E + \nu_{net}\, n$$

Approximate ∇μ and ∇n collinear with E with opposite sign

$$0 = -\mu |\nabla n| E - n |\nabla \mu| E + \nu_{net}\, n$$

Assume μ constant around 3MV/m (μ' = 0.05)
Assume ν linear around 3MV/m (ν' = 500(E-3E6)) = m(E-E_o)

$$\nabla \mu \xrightarrow{\text{constant}} 0$$

$$0 = -\mu' |\nabla n| E + m(E - E_o) n$$

$$-\mu'^{|\nabla n|} E + mnE = mnE_o$$

$$\frac{E_o}{E} - 1 = -\frac{\mu'}{m} \frac{|\nabla n|}{n}$$

@ E = E_o:

$$|\nabla n| \to 0$$

@ E > E_o:

$$\frac{|\nabla n|}{n} > 0$$

@ E < E_o:

$$\frac{|\nabla n|}{n} < 0 \to non - physical$$

B. *Plasma Frequency Derivation*

Assume a TEM wave:

$$E_x = E_o \cos(kz - \omega t)$$

$$F = ma = m\frac{d^2x}{dt^2} = eE_x$$

$$m\frac{d^2x}{dt^2} = eE_o \cos(kz - \omega t)$$

$$\frac{dx}{dt} = -\frac{eE_o}{m\omega} \sin(kz - \omega t)$$

$$x = -\frac{eE_o}{m\omega^2} \cos(kz - \omega t)$$

The electric dipole of an electron with displacement x is

$$p_x = -ex$$

The electric dipole of the electron density n_e is

$$P_x = -n_e e x$$

$$P_x = -\frac{n_e e^2 E_o}{m\omega^2} \cos(kz - \omega t)$$

The wave equations for and electromagnetic wave from Maxwell are:

$$\frac{\partial E_x}{\partial t} = -\frac{1}{\varepsilon_o}\left(\frac{\partial P_x}{\partial t} + \frac{\partial H_y}{\partial z}\right)$$

$$\frac{\partial H_y}{\partial t} = -\frac{1}{\mu_o}\frac{\partial E_x}{\partial z}$$

Solving for H_y in the second wave equation given

$$H_y = \frac{k}{\omega \mu_o} E_o \cos(kz - \omega t)$$

Substituting E_x, H_y, and P_x into the first wave equation given

$$\frac{\partial}{\partial t} E_o \cos(kz - \omega t) = -\frac{1}{\varepsilon_o}\left(\frac{\partial}{\partial t} - \frac{n_e e^2 E_o}{m\omega^2} \cos(kz - \omega t) + \frac{\partial}{\partial z}\frac{k}{\omega \mu_o} E_o \cos(kz - \omega t)\right)$$

Cancelling out the E_0sin(kz-ωt) terms after differenctiating

$$\omega = \frac{n_e e^2}{m\omega\varepsilon_o} + \frac{k^2}{\omega \mu_o \varepsilon_o}$$

$$\omega^2 = \frac{n_e e^2}{m\omega\varepsilon_o} + \frac{k^2}{\omega \mu_o \varepsilon_o}$$

$$\omega^2 = {\omega_p}^2 + k^2 c^2 \xrightarrow{yields} \omega_p = \sqrt{\frac{n_e e^2}{m\varepsilon_o}}$$

VIII. Bibliography

[1] J. See, W. Carr, and S. E. Collier, "Real time distribution analysis for electric utilities," in *Rural Electric Power Conference, 2008 IEEE*, 2008, p. B5–B5.

[2] C. R. Valenta, P. A. Graf, M. S. Trotter, G. A. Koo, G. D. Durgin, and B. J. Schafer, "Backscatter Channel Measurements at 5.8 GHz Across High-Voltage Corona," presented at the IEEE Sensors 2010, Hilo, HI, 2010.

[3] E. Nasser, *Fundamentals of Gaseous Ionization and Plasma Electronics*. New York: Wiley-Interscience, 1971.

[4] J. J. Clade, C. H. Gary, and C. A. Lefevre, "Calculation of corona losses beyond the critical gradient in alternating voltage," *Power Apparatus and Systems, IEEE Transactions on*, no. 5Part-I, p. 695–703, 2007.

[5] R. T. Waters, T. E. S. Rickard, and W. B. Stark, "Direct measurement of electric field at line conductors during a.c. corona," *Proc. IEE*, vol. 119, no. 6, pp. 717-723, Jun. 1972.

[6] J. S. Carroll and J. T. Lusignan, "The space charge that surrounds a conductor in corona," *American Institute of Electrical Engineers, Transactions of the*, vol. 47, no. 1, p. 50–57, 2009.

[7] F. W. Peek, *Determination Phenomena in High Voltage Engineering*. New York: McGraw-Hill, 1929.

[8] R. Fante, "Mathematical analysis of microwave breakdown in flowing gases," *Antennas and Propagation, IEEE Transactions on*, vol. 13, no. 5, p. 781–788, 1965.

[9] W. O. Price, J. Drapala, D. V. Thiel, and R. G. Olsen, "Corona Onset Voltage at 60 Hz and at High Frequency for an Isolated Cylindrical Monopole," *IEEE Transactions on Electromagnetic Compatibility*, vol. 50, no. 3, pp. 476-484, 2008.

[10] D. K. Davies and P. J. Chantry, "Air Chemistry Measurements II." Westinghouse R&D Center, Jul-1984.

[11] H. B. Wahlin, *The Motion of Electrons In Nitrogen*. Madison, WI: University of Wisconsin, 1923.

[12] A. E. Rodriguez, W. L. Morgan and K. J. Touryan and W. M. Moeny, , and , T. H. Martin, "An air breakdown kinetic model," *Journal of Applied Physics*, vol. 70, no. 4, pp. 2015-2022, Aug. 1991.

[13] J. Chen and J. H. Davidson, "Electron density and energy distributions in the positive DC corona: interpretation for corona-enhanced chemical reactions," *Plasma Chemistry and Plasma Processing*, vol. 22, no. 2, p. 199–224, 2002.

[14] L. Wei, Q. Jinghui, D. Weibo, and S. Ying, "Research on an axially slotted cylinder antenna coated with plasma sheath," in *Microwave and Millimeter Wave Technology, 2008. ICMMT 2008. International Conference on*, vol. 4, p. 1875–1878.

[15] M. A. Lieberman and A. J. Lichtenberg, *Principles of Plasma Discharges and Materials Processing*. New York: Wiley, 1994.

[16] M. Laroussi, "Interaction of microwaves with atmospheric pressure plasmas," *International journal of infrared and millimeter waves*, vol. 16, no. 12, p. 2069–2083, 1995.

[17] M. Laroussi and W. T. Anderson, "Attenuation of electromagnetic waves by a plasma layer at atmospheric pressure," *International journal of infrared and millimeter waves*, vol. 19, no. 3, p. 453–464, 1998.

[18] J. Chen and J. H. Davidson, "Ozone production in the positive DC corona discharge: Model and comparison to experiments," *Plasma chemistry and plasma processing*, vol. 22, no. 4, p. 495–522, 2002.

[19] J. Chen and J. H. Davidson, "Ozone production in the positive DC corona discharge: Model and comparison to experiments," *Plasma chemistry and plasma processing*, vol. 22, no. 4, p. 495–522, 2002.